CH_3CN Insertion Reactions of $(C_5H_4R)_2Zr(R)(L)^+$ Complexes

Yun W. Alelyunas, Richard F. Jordan,* Scott F. Echols, Samuel L. Borkowsky, and Prudence K. Bradley

Department of Chemistry, University of Iowa, Iowa City, Iowa 52242

Received October 5, 1990

The cationic complexes $Cp_2Zr(R)(CH_3CN)_n^+$ (R = H, Ph, CH_3, η^2-CH_2Ph), generated by ligand substitution of $Cp_2Zr(R)(THF)^+$ or by reaction of Cp_2ZrR_2 with Ag^+ or Cp'_2Fe^+ in CH_3CN, undergo single, irreversible CH_3CN insertion to yield the azaalkenylidene complexes $Cp_2Zr\{N{=}C(R)(CH_3)\}(CH_3CN)^+$. The qualitative trend in migratory aptitude is H, Ph (rapid at 23 °C) ≫ CH_3 ≫ η^2-CH_2Ph (no reaction at 60 °C). NMR and kinetic studies of $(C_5H_4R)_2Zr(CH_3)(CH_3CN)_n^+$ (R = H, CH_3) complexes in CD_2Cl_2 solution establish that the bis-CH_3CN adducts (n = 2) are strongly favored vs the mono-CH_3CN adducts and undergo insertion. A slight apparent rate inhibition by added CH_3CN is ascribed to a solvent effect. Substitution of both Cp ligands of $Cp_2Zr(CH_3)(CH_3CN)_2^+$ by C_5H_4Me increases the insertion rate by a factor of 3. This is ascribed to more effective stabilization of the developing electron deficiency at the metal in the transition state leading from the 5-coordinate reactant to the 4-coordinate product by the better donor C_5H_4Me ligands.

Introduction

Recent investigations of the synthesis and reaction chemistry of d^0 Cp^*_2MR,[1] Cp_2MR^+ and $Cp^*_2MR^+$,[2] and $Cp_2M(R)(L)_n^+$ complexes (Cp = η^5-C_5H_5; Cp* = η^5-C_5Me_5),[3-5] ESCA studies on Cp_2MX_2/aluminoxane catalysts,[6] and detailed studies of polypropylene stereochemistry[7] provide support for the earlier proposal that cationic d^0 alkyl compounds Cp_2MR^+ are active species in metallocene-based Ziegler–Natta olefin polymerization catalyst systems.[8] The reactions of isolable $Cp_2Zr(R)(L)^+$ compounds with unsaturated substrates are of interest for (i) understanding the factors that influence the rates of insertion and β-H elimination reactions, and hence chain-propagation and chain-transfer reactions in polymerization processes,[1d] and (ii) developing applications of these systems in other stoichiometric and catalytic C–C bond-forming reactions.[9,10]

Scheme I

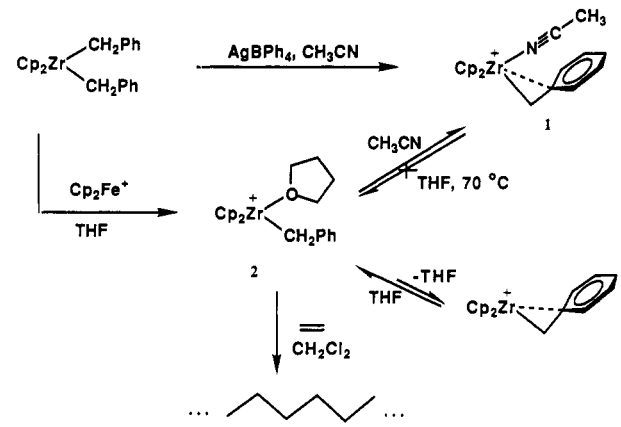

Bochmann has studied the scope and mechanisms of nitrile insertion reactions of $Cp_2Ti(CH_3)(RCN)^+$ and $(Ind)_2Ti(CH_3)(RCN)^+$ (Ind = indenyl) complexes (eq 1).[11] Kinetic studies show that these reactions proceed by rate-limiting alkyl migration to the coordinated nitrile, yielding the azaalkenylidene intermediate [TiN=C(R)-(Me)], which is rapidly trapped by a second equivalent of nitrile. Similar insertion reactions have been observed for $[Cp_2Y(H)(THF)]_2$, $Cp^*_2Y(R)$, and $Cp^*_2Sc(R)$ complexes, as well as for several other metal hydride and alkyl systems.[12-15]

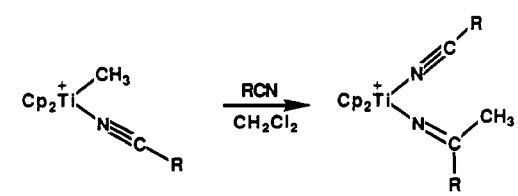

(1)

(1) (a) Watson, P. L.; Parshall, G. W. *Acc. Chem. Res.* **1985**, *18*, 51. (b) Watson, P. L. *J. Am. Chem. Soc.* **1982**, *107*, 8091. (c) Jeske, G.; Lauke, H.; Mauermann, H.; Sweptson, P. N.; Schumann, H.; Marks, T. J. *J. Am. Chem. Soc.* **1985**, *107*, 8091. (d) Burger, B. J.; Thompson, M. E.; Cotter, W. D.; Bercaw, J. F. *J. Am. Chem. Soc.* **1990**, *112*, 1566. (e) See also: Crowther, D. J.; Baenziger, N. C.; Jordan, R. F. *J. Am. Chem. Soc.* **1991**, *113*, 1455.

(2) (a) Eisch, J. J.; Piotrowski, A. M.; Brownstein, S. K.; Gabe, E. J.; Lee, F. L. *J. Am. Chem. Soc.* **1985**, *107*, 7219. (b) Hlatkey, G. G.; Turner, H. W.; Eckman, R. R. *J. Am. Chem. Soc.* **1989**, *111*, 2798. (c) Christ, C. S., Jr.; Eyler, J. R.; Richardson, D. E. *J. Am. Chem. Soc.* **1990**, *112*, 596. (d) Bochmann, M.; Jaggar, A. J.; Nicholls, J. C. *Angew. Chem., Int. Ed. Engl.* **1990**, *29*, 780.

(3) (a) Jordan, R. F.; Dasher, W. E.; Echols, S. F. *J. Am. Chem. Soc.* **1986**, *108*, 1718. (b) Jordan, R. F.; Bajgur, C. S.; Willett, R.; Scott, B. *J. Am. Chem. Soc.* **1986**, *108*, 7410. (c) Jordan, R. F.; LaPointe, R. E.; Bajgur, C. S.; Willett, R. *J. Am. Chem. Soc.* **1987**, *109*, 4111. (d) Jordan, R. F.; Bajgur, C. S.; Dasher, W. E.; Rheingold, A. L. *Organometallics* **1987**, *6*, 1041. (e) Jordan, R. F.; Echols, S. F. *Inorg. Chem.* **1987**, *26*, 383. (f) Jordan, R. F. *J. Chem. Educ.* **1988**, *65*, 285. (g) Jordan, R. F.; Bradley, P. F.; LaPointe, R. E.; Taylor, D. F. *New J. Chem.* **1990**, *14*, 505. (h) Jordan, R. F.; LaPointe, R. E.; Bradley, P. K.; Baenziger, N. *Organometallics* **1989**, *8*, 2892. (i) Jordan, R. F.; Bradley, P. K.; LaPointe, R. E.; Baenziger, N. *J. Am. Chem. Soc.* **1990**, *112*, 1289. (j) Jordan, R. F.; LaPointe, R. E.; Baenziger, N.; Hinch, G. D. *Organometallics* **1990**, *9*, 1539.

(4) (a) Bochmann, M.; Wilson, L. M.; Hursthouse, M. B.; Short, R. L. *Organometallics* **1987**, *6*, 2556. (b) Taube, R.; Krukowa, L. *J. Organomet. Chem.* **1988**, *347*, C9.

(5) Lin, Z.; LeMarechal, J.-F.; Sabat, M.; Marks, T. J. *J. Am. Chem. Soc.* **1987**, *109*, 4127.

(6) Gassman, P. G.; Callstrom, M. R. *J. Am. Chem. Soc.* **1987**, *109*, 7875.

(7) (a) Ewen, J. A. *J. Am. Chem. Soc.* **1984**, *106*, 6355. (b) Ewen, J. A.; Jones, R. L.; Razavi, A.; Ferrara, J. D. *J. Am. Chem. Soc.* **1988**, *110*, 6255. (c) Pino, P.; Cioni, P.; Wei, J. *J. Am. Chem. Soc.* **1987**, *109*, 6189. (d) Zambelli, A.; Longo, P.; Grassi, A. *Macromolecules* **1989**, *22*, 2186.

(8) (a) Zefirova, A. K.; Shilov, A. E. *Dokl. Akad. Nauk SSSR* **1961**, *136*, 599. (b) Dyachkovskii, F. S.; Shilova, A. K.; Shilov, A. E. *J. Polym. Sci., Part C* **1967**, *16*, 2333. (c) Long, W. P.; Breslow, D. S. *J. Am. Chem. Soc.* **1960**, *82*, 1953. (d) Breslow, D. S.; Newburg, N. R. *J. Am. Chem. Soc.* **1959**, *81*, 81.

(9) Jordan, R. F.; Taylor, D. F. *J. Am. Chem. Soc.* **1989**, *111*, 778.

(10) (a) Jordan, R. F.; Taylor, D. F.; Baenziger, N. C. *Organometallics* **1990**, *9*, 1546. (b) Jordan, R. F.; Guram, A. S. *Organometallics* **1990**, *9*, 2116. (c) Guram, A. S.; Jordan, R. F. *Organometallics* **1990**, *9*, 2190. (d) Guram, A. S.; Jordan, R. F.; Taylor, D. F. *J. Am. Chem. Soc.* **1991**, *113*, 1833.

(11) Bochmann, M.; Wilson, L. M.; Hursthouse, M. B.; Motevalli, M. *Organometallics* **1988**, *7*, 1148.

(12) den Haan, K. H.; Luinstra, G. A.; Meetsma, A.; Teuben, J. H. *Organometallics* **1987**, *6*, 1509.

(13) Evans, W. J.; Meadows, J. H.; Hunter, W. E.; Atwood, J. L. *J. Am. Chem. Soc.* **1984**, *106*, 1291.

0276-7333/91/2310-1406$02.50/0

In contrast, neither four-coordinate d^0 alkyls such as $Cp_2M(R)(X)$ and $Cp^*_2MR_2$ (M = Ti, Zr) nor the d^1 complexes $Cp_2Ti(R)$ insert nitriles under mild conditions, though the latter form nitrile adducts.[16,17] Aluminum alkyls coordinate and insert nitriles; however, if β-hydrogens are present in the Al–R groups, elimination of olefin and insertion of the nitrile into the resulting Al–H bond is observed.[18] For example, the reaction of $AlEt_3$ with ^{t}BuCN produces primarily ethylene and $[Et_2AlN{=}C(^t Bu)(H)]_2$. If the nitrile contains α-hydrogens, more complex reactions involving metalation of the nitrile occur.[18,19a] C–H activation is also observed in the reactions of d^0 $Cp_2^*LnCH(SiMe_3)_2$ complexes (Ln = La, Ce) with CH_3CN.[19b]

We noted earlier that the cationic hydrides $Cp_2Zr(H)(THF)^+$ and $Cp'_2Zr(H)(THF)^+$ ($Cp' = \eta^5$-C_5H_4Me) react rapidly (upon dissolution) at ambient temperature in CH_3CN to yield the cationic azaalkenylidene complexes $(C_5H_4R)_2Zr\{N{=}C(H)(Me)\}(CH_3CN)^+$ (R = H, Me).[3d,h,20] We also noted that the analogous methyl complex $Cp_2Zr(CH_3)(THF)^+$ undergoes a similar but slower insertion to yield $Cp_2Zr\{N{=}C(Me)_2\}(CH_3CN)^+$.[3d] These initial observations prompted a more thorough study of the scope and mechanisms of the reactions of $Cp_2Zr(R)(L)^+$ complexes with the model unsaturated substrate CH_3CN. In this paper, the CH_3CN insertion reactions of $Cp_2Zr(R)(L)^+$ and $Cp'_2Zr(R)(L)^+$ complexes (R = H, CH_3, Ph, CH_2Ph) are discussed. This series was studied to elucidate the trend in R migratory aptitude and to determine the effect of Cp electron-donor ability on the insertion rate. The CH_3CN chemistry of $Cp'_2Zr(R)(L)^+$ complexes that contain β-hydrogens is discussed in a subsequent paper.[21]

Results

Synthesis and Reactivity of $Cp_2Zr(CH_2Ph)(L)^+$ Complexes. We reported in a preliminary communication that the cationic benzyl complex $Cp_2Zr(\eta^2$-$CH_2Ph)(CH_3CN)^+$ (1) is formed via reaction of $Cp_2Zr(CH_2Ph)_2$ with $Ag[BPh_4]$ in CD_3CN (Scheme I).[3c] Complex 1 is moderately soluble in CH_3CN and THF and, surprisingly, can be recrystallized from the latter solvent without substitution of the CH_3CN. However, in CD_2Cl_2 solvent, exchange of coordinated and free CH_3CN is rapid on the NMR time scale. The X-ray structure of 1 reveals the presence of a distorted benzyl ligand with an acute Zr–C–C angle (84.9 (4)°), an elongated Zr–CH_2 bond (2.344 (8) Å), and a close Zr–Ph contact (Zr–C_{ipso} distance 2.648 (6) Å).[3c] High-field (relative to $Cp_2Zr(CH_2Ph)_2$) ^{1}H NMR resonances for the ortho hydrogens (δ 6.75) and ^{13}C NMR resonances for the methylene (δ 44.1) and ipso (δ 126.0) carbons, and an unusually large J_{CH} value for the methylene carbon (145 Hz), establish that this η^2 structure is maintained in CH_3CN solution.[22] Similar η^2 or η^n structures have been observed for other unsaturated d^0 and d^0f^n metal benzyl complexes.[23] The cationic benzyl complex 1 is resistant to CH_3CN insertion, remaining unchanged after 5 h at 60 °C in CD_3CN solution.

The THF complex $Cp_2Zr(CH_2Ph)(THF)^+$ (2) is not accessible from 1 but can be prepared directly by reaction of $Cp_2Zr(CH_2Ph)_2$ with $[Cp'_2Fe][BPh_4]$ in THF (Scheme I).[3c] The absence of high-field ortho hydrogen resonances in the ^{1}H NMR spectrum of 2 establishes that this complex has a normal η^1-benzyl ligand. Complex 2 is not sufficiently soluble for ^{13}C NMR analysis. The difference in the structures of 1 and 2 is likely due to the bonding modes of the CH_3CN and THF ligands. While the CH_3CN ligand in 1 is a $2e^-$ σ donor, π-donation from the potentially $4e^-$ donor THF ligand in 2 would utilize the vacant Zr orbital required for η^2-benzyl bonding.[3d,i]

Complex 2 catalyzes the polymerization of ethylene (1 atm, CD_2Cl_2, 23 °C). Low-temperature ^{1}H NMR monitoring of CD_2Cl_2 solutions of 2 allows observation of the "naked" benzyl species $Cp_2Zr(\eta^2$-$CH_2Ph)^+$ (or its CD_2Cl_2 solvate) formed by THF dissociation from 2.[3f] Ethylene polymerization likely proceeds by coordination of ethylene to $Cp_2Zr(\eta^2$-$CH_2Ph)^+$ followed by insertion. The observation of polymerization catalysis by 2 suggests that Zr–CH_2Ph bonds are not inherently unreactive in insertions.

Synthesis of $(C_5H_4R)_2Zr\{N{=}C(Me)(Ph)\}(L)^+$ Complexes (R = H, CH_3): CH_3CN Insertion of $(C_5H_4R)_2Zr(Ph)(CH_3CN)_n^+$. The reaction of Cp_2ZrPh_2 with $Ag[BPh_4]$ in CH_3CN solution at 23 °C yields directly the cationic CH_3CN insertion product $Cp_2Zr\{N{=}C(Me)(Ph)\}(CH_3CN)^+$ (3, >95% NMR, 45% isolated, eq 2). Complex 3 is also produced by reaction of Cp_2ZrPh_2 with $[Cp_2Fe][BPh_4]$ in CH_3CN (eq 2). As Cp_2ZrPh_2 does not react with CH_3CN under these conditions, these reactions most likely yield initially the cationic phenyl complex $Cp_2Zr(Ph)(CH_3CN)_n^+$, which inserts CH_3CN. When these reactions are monitored by ^{1}H NMR spectroscopy, only Cp_2ZrPh_2 and 3 are observed, indicating that the insertion is rapid at 23 °C. This is confirmed by the reaction of $Cp_2Zr(Ph)(THF)^+$ in CD_3CN, which proceeds rapidly (upon dissolution) via ligand substitution and insertion to yield $Cp_2Zr\{N{=}C(CD_3)(Ph)\}(CD_3CN)^+$ (3-d_6).[24] Charac-

(14) Bercaw, J. E.; Davies, D. L.; Wolczanski, P. T. *Organometallics* **1986**, *5*, 443.
(15) (a) Anderson, R. A.; Simpson, S. J. *J. Am. Chem. Soc.* **1981**, *103*, 4063. (b) Churchill, M. R.; Wasserman, H. J.; Belmonte, P. A.; Schrock, R. R. *Organometallics* **1982**, *1*, 559. (c) Cramer, R. E.; Panchanatheswaran, K.; Gilje, J. W. *J. Am. Chem. Soc.* **1984**, *104*, 1853. (d) Richeson, D. S.; Mitchell, J. F.; Theopold, K. H. *J. Am. Chem. Soc.* **1987**, *109*, 5868. (e) Sternal, R. S.; Sabat, M.; Marks, T. J. *J. Am. Chem. Soc.* **1987**, *109*, 7920. (f) Dormond, A.; Aaliti, A.; Elbonadili, A.; Moise, C. *J. Organomet. Chem.* **1987**, *329*, 187. (g) McGilligan, B. S.; Wright, T. C.; Wilkinson, G.; Motevalli, M.; Hursthouse, M. B. *J. Chem. Soc., Dalton Trans.* **1988**, 1737. (h) Richeson, D. S.; Mitchell, J. F.; Theopold, K. H. *Organometallics* **1989**, *8*, 2570. (i) Dormond, A.; Elbonadili, A.; Moise, C. *J. Org. Chem.* **1989**, *54*, 3747. (j) Doxsee, K. M.; Farahi, J. B. *J. Am. Chem. Soc.* **1988**, *110*, 7239.
(16) (a) Collier, M. F.; Lappert, M. F.; McMeeking, *J. Inorg. Nucl. Chem. Lett.* **1971**, *7*, 689. (b) Negishi, E.; Takahashi, T. *Aldrichim. Acta* **1985**, *18*, 31. (c) de Boer, E. J. M.; Teuben, J. H. *J. Organomet. Chem.* **1977**, *140*, 41. (d) de Boer, E. J. M.; Teuben, J. H. *J. Organomet. Chem.* **1978**, *153*, 53.
(17) However, neutral Cp_2M hydride, allyl, benzyne, and related complexes insert/couple with nitriles. For example, see: (a) Erker, G.; Fromberg, W.; Atwood, J. L.; Hunter, W. E. *Angew. Chem., Int. Ed. Engl.* **1984**, *23*, 68. (b) Klei, E.; Teuben, J. H.; de Liefde Meijer, H. J. *J. Chem. Soc., Chem. Commun.* **1981**, 342. (c) Buchwald, S. L.; Nielsen, R. B. *Chem. Rev.* **1988**, *88*, 1047. (d) Yasuda, H.; Nakamura, A. *Angew. Chem., Int. Ed. Engl.* **1987**, *26*, 723. (e) Fisher, R. A.; Buchwald, S. L. *Organometallics* **1990**, *9*, 871.
(18) (a) For a review see: Zietz, J. R., Jr.; Robinson, G. C.; Lindsay, K. L. In *Comprehensive Organometallic Chemistry*; Wilkinson, G., Stone, F. G. A., Abel, E. W., Eds.; Pergamon Press: Oxford, U.K., 1982; Vol. 7, p 431. (b) Lloyd, J. E.; Wade, K. *J. Chem. Soc.* **1965**, 2662. (c) Jennings, J.; Lloyd, J. E.; Wade, K. *J. Chem. Soc.* **1965**, 5083. (d) Ziegler, K.; Schneider, K.; Schneider, J. *Justus Liebigs Ann. Chem.* **1959**, *623*, 9.
(19) (a) Pasynkiewicz, S.; Kuran, W.; Zbierchowska, A. *Justus Liebigs Ann. Chem.* **1975**, 636. (b) Heeres, H. J.; Meetsma, A.; Teuben, J. H. *Angew. Chem., Int. Ed. Engl.* **1990**, *29*, 420.
(20) All cationic complexes in this paper are studied as the BPh_4^- salts.
(21) Alelyunas, Y. W.; Jordan, R. F.; LaPointe, R. E., manuscript in preparation.
(22) Latesky, S. L.; McMullen, A. K.; Niccolai, G. P.; Rothwell, I. P.; Huffman, J. C. *Organometallics* **1985**, *4*, 902.
(23) (a) Davies, G. R.; Jarvis, J. A. J.; Kilbourn, B. T.; Pioli, A. J. P. *J. Chem. Soc. D* **1971**, 677. (b) Davies, G. R.; Jarvis, J. A. J.; Kilbourn, B. T. *J. Chem. Soc. D* **1971**, 1511. (c) Bassi, I. W.; Allegra, G.; Scordamaglia, R.; Chioccola, G. *J. Am. Chem. Soc.* **1971**, *93*, 3787. (d) Mintz, E. A.; Moloy, K. G.; Marks, T. J.; Day, V. W. *J. Am. Chem. Soc.* **1982**, *104*, 4692. (e) Edwards, P. G.; Andersen, R. A.; Zalkin, A. *Organometallics* **1984**, *3*, 293. (f) Girolami, G. S.; Wilkinson, G.; Thornton-Pett, M.; Hursthouse, M. B. *J. Chem. Soc., Dalton Trans.* **1984**, 2789. (g) Scholz, J.; Schlegel, M.; Thiele, K.-H. *Chem. Ber.* **1987**, *120*, 1369.

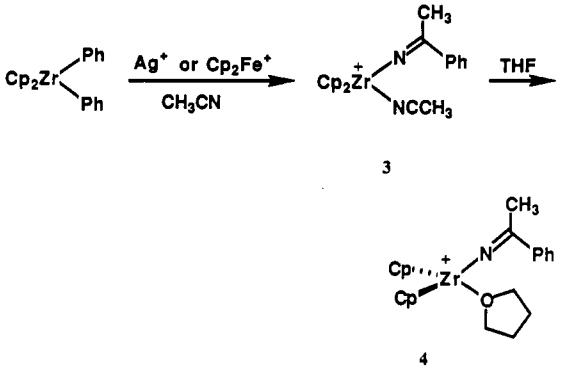

3

4 (2)

teristic spectral parameters for **3** include a low-field ^{13}C NMR resonance (δ 176) for the imino carbon and an IR $\nu_{C=N}$ absorbance at 1655 cm^{-1}. Reaction of **3** with neat THF yields the THF complex $Cp_2Zr\{N{=}C(Me)(Ph)\}(THF)^+$ (**4**), which was isolated by crystallization from THF/Et_2O and characterized by ^1H NMR spectroscopy and elemental analysis.

The reaction of Cp'_2ZrPh_2 with $Ag[BPh_4]$ in CH_3CN at 23 °C produces $Cp'_2Zr\{N{=}C(Me)(Ph)\}(CH_3CN)^+$ (**5**: IR $\nu_{C=N}$ 2310, 2280 cm^{-1}; $\nu_{N=C}$ 1650 cm^{-1}). Thus, as observed for the Cp_2Zr case, the intermediate $Cp'_2Zr(Ph)(CH_3CN)^+$ must undergo rapid CH_3CN insertion.

Reaction of $(C_5H_4R)_2Zr(CH_3)(THF)^+$ (R = H, CH_3) Complexes with CH_3CN. We reported previously that dissolution of $Cp_2Zr(CH_3)(THF)^+$ (**6**) in CH_3CN yields the isolable bis(acetonitrile) complex $Cp_2Zr(CH_3)(CH_3CN)_2^+$ (**7**) and free THF (eq 3).[3d] In CH_3CN solution at 23–40 °C, **7** rearranges to the insertion product $Cp_2Zr(N{=}CMe_2)(CH_3CN)^+$ (**8**, >90% yield by NMR analysis, eq 4).

$$Cp_2Zr(CH_3)(THF)^+ \xrightarrow[-\ THF]{CH_3CN} Cp_2Zr(CH_3)(NCCH_3)_2^+ \quad (3)$$

6 7

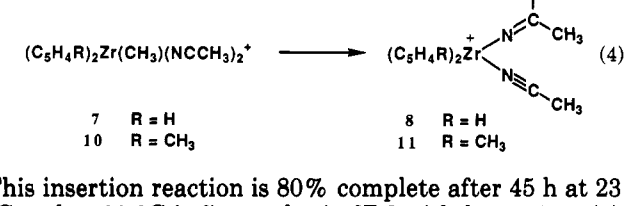

7 R = H; 10 R = CH_3 8 R = H; 11 R = CH_3 (4)

This insertion reaction is 80% complete after 45 h at 23 °C and at 30 °C is first order in [Zr] with k_{obs} = 2.13 (7) × 10^{-5} s^{-1}. Complex **8** was isolated by crystallization from cold CH_3CN/Et_2O and characterized by NMR and IR spectroscopy and elemental analysis. Key spectroscopic features include the expected low-field ^{13}C NMR resonance for the imino carbon at δ 180.9 and IR $\nu_{C=N}$ (2300, 2270 cm^{-1}) and $\nu_{C=N}$ (1680 cm^{-1}) absorbances. Complex **8** is stable at room temperature but decomposes above 50 °C to produce a mixture that was not characterized.[25]

Similarly, the C_5H_4Me derivative $Cp'_2Zr(CH_3)(THF)^+$ (**9**), which is prepared by reaction of $Cp'_2Zr(CH_3)_2$ with Cp'_2Fe^+, reacts with neat CH_3CN to yield the thermally sensitive bis(acetonitrile) adduct $Cp'_2Zr(CH_3)(CH_3CN)_2^+$ (**10**) and free THF. The ^1H NMR spectrum of $Cp'_2Zr(CH_3)(CD_3CN)_2^+$ (**10**-d_6), generated by dissolution of **9** in CD_3CN, exhibits a $Zr-CH_3$ resonance at δ 0.01, shifted upfield by 0.64 ppm from the $Zr-CH_3$ resonance of **9** (in CD_2Cl_2). This is similar to the upfield shift of the $Zr-CH_3$ resonance observed upon conversion of the Cp_2Zr analogue **6** to **7**.[3d] Complex **10** rearranges at 23 °C in CH_3CN solution, or CD_2Cl_2 solution in the presence of excess CH_3CN, to the insertion product **11** (>95% yield by NMR analysis, 75% isolated yield, eq 4). No side reactions (e.g. Cl^- abstraction in CD_2Cl_2) are observed at the NMR detection limit (<5%).[26] The spectroscopic properties of complex **11** are analogous to those of **8**.

Solution Behavior of Nitrile Adducts 7 and 10. Low-temperature ^1H NMR spectra of the bis(acetonitrile) complex **7** (−98 °C, THF-d_8) show that it exists as a mixture of two isomers which differ in the position of the CH_3 group (central or outer coordination site in the plane between the two Cp ligands).[3d] The Cp (δ 6.16, 6.10) and $Zr-CH_3$ (δ 0.05) resonances for both isomers are nearly identical under these conditions. Isomer exchange is rapid on the NMR time scale in CD_2Cl_2 or CD_3CN solution at 30 °C. In CD_3CN solution, the $Zr-CH_3$ resonance for **7** appears at δ 0.08.[3a,d] The CH_3CN ligands of **7** are labile (eq 5). In the solid state, **7** loses CH_3CN under vacuum

$$(C_5H_4R)_2Zr(CH_3)(NCCH_3)_2^+ \rightleftharpoons$$

7 R = H
10 R = CH_3

$$(C_5H_4R)_2Zr(CH_3)(NCCH_3)^+ + CH_3CN \quad (5)$$

to yield the mono(acetonitrile) adduct $Cp_2Zr(CH_3)(CH_3CN)^+$.[3a,d] This complex is sparingly soluble and unstable in CD_2Cl_2 so that only low-resolution ^1H NMR spectra are obtained; these show a $Zr-CH_3$ chemical shift of δ 0.68. Complex **7** also undergoes rapid exchange (on the NMR time scale) with free CH_3CN or CD_3CN in CD_2Cl_2 or CD_3CN solution. However, the extent of CH_3CN dissociation from **7** at 30 °C is very small. The $Zr-CH_3$ chemical shift of **7** in CD_2Cl_2 solutions containing added CD_3CN is insensitive to $[CD_3CN]$ and nearly equal to that in neat CD_3CN. For example, increasing $[CD_3CN]$ from 0.5 to 3.1 M results in a shift of the $Zr-CH_3$ resonance from δ 0.14 to 0.11, only a net 0.03 ppm change. Assuming that (i) this change is due to the equilibrium in eq 5 and that (ii) the effect of solvent polarity on the chemical shift is negligible, and noting that $\delta(Zr-CH_3)$ for the monoadduct is 0.68, K_{eq} may be estimated to be <0.036 (5) M at 30 °C (see Experimental Section). This estimate is an upper limit for K_{eq}, since changes in the solvent composition may contribute to the change in chemical shift (e.g. increasing $[CD_3CN]$ from 0.7 to 4.0 M results in a shift in one of the BPh_4^- resonance from δ 6.89 to 6.85, a net 0.04 ppm change).

The solution behavior of **10** is analogous to that of **7**. The ^1H NMR spectrum of isolated **10** at −40 °C in CD_2Cl_2 solution containing 1.8 M excess CD_3CN to inhibit insertion (vide infra) exhibits a $Zr-CH_3$ resonance at δ 0.01 and a resonance for free CH_3CN (δ 1.97) that is integrated for 6 H. The latter establishes that isolated **10** contains two CH_3CN ligands which are labile. Complex **10** undergoes exchange with free CH_3CN rapidly on the NMR time scale in CD_2Cl_2 solution. Exposure of solid **10** to vacuum yields a mixture of the mono(acetonitrile) adduct $Cp'_2Zr(CH_3)(CH_3CN)^+$ and insertion product **11**; i.e., insertion is competitive with CH_3CN loss in the solid state. For example, exposure of solid **10** to vacuum at 23 °C for 30 min, followed by dissolution in CD_2Cl_2, produces 59% of the monoadduct and 41% of **11** as shown by ^1H NMR spectroscopy at −80 °C. At 30 °C (CD_2Cl_2), the $Zr-CH_3$

(24) For the synthesis of $Cp_2Zr(Ph)(THF)^+$ see: Borkowsky, S. L.; Jordan, R. F.; Hinch, G. D. *Organometallics*, in press.

(25) Azaalkenylidene/nitrile coupling reactions have been observed in related Sc, Ti, and Cr systems.[14,16b,j]

(26) The chloride abstraction product $Cp'_2Zr(CH_3)Cl$ is synthesized (NMR tube reaction) from the reaction of $Cp'_2Zr(CH_3)(THF)^+$ with $[Me_4N]Cl$ ($[Me_4N]Cl$ is slightly soluble and the product $[Me_4N][BPh_4]$ is insoluble in CD_2Cl_2). ^1H NMR (CD_2Cl_2): δ 6.07 (m, 2 H, C_5H_4), 5.97 (m, 6 H, C_5H_4), 2.19 (m, 6 H, $C_5H_4CH_3$), 0.16 (s, 3 H, $Zr-CH_3$).

resonance of the mono(acetonitrile) complex $Cp'_2Zr(CH_3)(CH_3CN)^+$ appears at δ 0.59. As for **7**, the extent of CH_3CN dissociation from **10** at 30 °C is small. The Zr–CH_3 resonance of **10** in CD_2Cl_2 solution is insensitive to added CD_3CN; increasing $[CD_3CN]$ from 1.0 to 3.9 M results in a shift of the Zr–CH_3 resonance from δ 0.13 to 0.05. With use of the assumptions noted above for **7**, K_{eq} (for eq 5) may be estimated to be <0.23 (2) M at 30 °C. The higher K_{eq} value for **10** (versus **7**) reflects the stronger electron-donating ability of Cp′ versus Cp.

Solution Structures of Cationic Zr Azaalkenylidene Complexes. X-ray structural results for $Cp_2Zr\{N{=}C(H)(Ph)\}Cl$[17a] and $[(Ind)_2Ti\{N{=}C(Me)(Ph)\}(PhCN)][BPh_4]$[11] establish that in each case the azaalkenylidene ligand lies in the plane between the two Cp or Ind ligands. In this "in-plane" orientation, Zr–N π-bonding is possible[27] and steric crowding involving the Cp ligands is minimized. NMR results on related compounds are also consistent with "in-plane" structures.[11-15] For unsymmetrical $(C_5H_4R)_2Zr\{N{=}C(R)(R')\}(L)^+$ complexes, two isomeric in-plane structures are possible, whereas for symmetrical $(C_5H_4R)_2Zr\{N{=}C(R)_2\}(L)^+$ complexes one isomer with inequivalent R groups is possible. Exchange between the two isomers in the former case, or exchange of the two inequivalent R groups in the latter case, could occur either by rotation about the Zr—N=C linkage or by L ligand exchange.

The 90-MHz ^1H NMR spectrum of $Cp_2Zr\{N{=}C(Me)(Ph)\}(THF)^+$ (**4**) in CD_2Cl_2 at 23 °C exhibits singlets for the Cp (δ 6.22) ligands and the imino Me (δ 2.39) group. In the 200-MHz spectrum of the same solution at −82 °C, these resonances are slightly shifted and appear as unequal (ca. 2/1) doublets (Cp δ 6.17, 6.16; Me δ 2.35, 2.40). These results establish that the azaalkenylidene ligand lies in the plane between the two Cp ligands as shown and that interconversion of the two possible "in-plane" isomers (one of which is slightly favored) is rapid on the 90-MHz NMR time scale at 23 °C. The NMR results in Table I indicate that for related Zr–Ph insertion products **3** and **5** the analogous exchange processes are also rapid at ambient T in CD_3CN.

NMR data establish that $Cp'_2Zr(N{=}CMe_2)(CH_3CN)^+$ (**11**) also exists in the expected "in-plane" structure but that rotation about the Zr—N=C linkage is slow on the NMR time scale. The ^1H and ^{13}C NMR spectra of **11** in CD_2Cl_2 solution (Table I) each contain two $N{=}C(CH_3)_2$ resonances, indicating that the $N{=}C(CH_3)_2$ groups are inequivalent, as expected in a static "in-plane" structure. Addition of CH_3CN or CD_3CN to **11** in CD_2Cl_2 results in collapse of the two $N{=}C(CH_3)$ ^1H resonances to a single resonance (δ 1.94), suggesting that the exchange is promoted by associative ligand exchange. ^1H NMR spectra of the Cp_2Zr analogue **8** in CD_3CN or CD_2Cl_2 solution (23 °C) exhibit a single $N{=}C(CH_3)_2$ resonance, indicating that the exchange of two inequivalent CH_3 groups is rapid.

Kinetics of CH_3CN Insertion Reactions of $(C_5H_4R)_2Zr(CH_3)(L)^+$ Complexes. The kinetics of the CH_3CN reactions of **7** and **10** (eq 4) in CD_2Cl_2 solvent have been studied by ^1H NMR spectroscopy for elucidation of the mechanism of these insertions and for comparison with Bochmann's studies of related cationic Ti systems.[11]

Solutions of the CD_3CN adducts **7**-d_6 and **10**-d_6 in CD_2Cl_2 were prepared in situ in NMR tubes by addition of excess CD_3CN (>20 equiv vs Zr, quantified by gas bulb measurements) to solutions of the THF complexes **6** and **9**. In these experiments CD_3CN rather than CH_3CN was used to simplify the NMR spectra and to avoid dynamic range problems that make accurate peak integration difficult. Low-temperature (−40 °C) ^1H NMR spectra of such solutions exhibit single Zr–CH_3 resonances shifted upfield by ca. 0.6 ppm from the resonances of **6** or **9** (close to the resonances for the bis(acetonitrile) complexes in CD_3CN solution) and resonances for free THF[28] that do not change during the course of the subsequent insertion reactions. These results indicate that in both cases complete displacement of THF by CD_3CN occurs under these conditions.

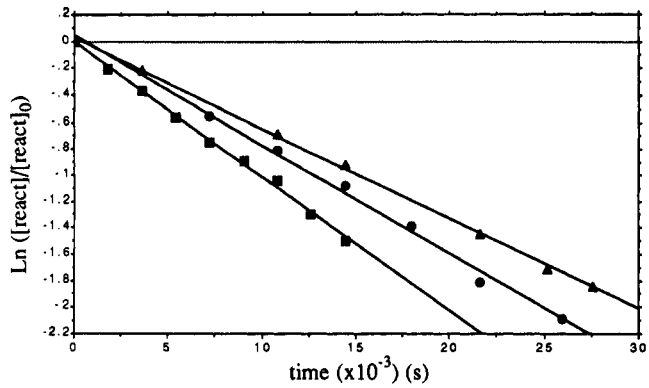

Figure 1. Pseudo-first-order plots for disappearance of **10**-d_6 in the presence of varying $[CD_3CN]$: (■) $[CD_3CN]$ = 0.94 M; (●) $[CD_3CN]$ = 1.72 M; (▲) $[CD_3CN]$ = 3.58 M.

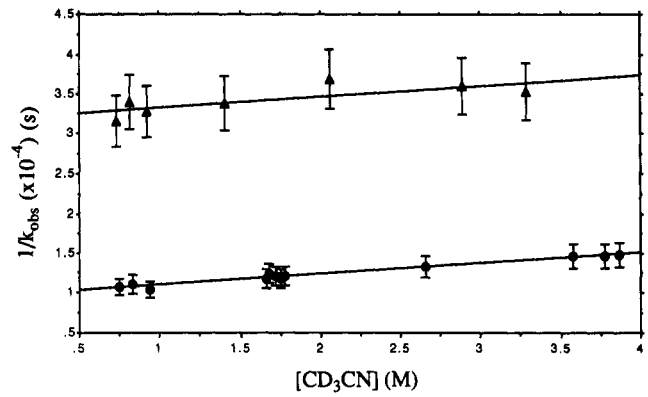

Figure 2. Plots of $1/k_{obs}$ (in CD_2Cl_2/CD_3CN mixed solvent) vs $[CD_3CN]$: (▲) data for complex **7**-d_6; (●) data for complex **10**-d_6.

Thermolyses were carried out at 30.2 ± 0.4 °C over a range of $[CD_3CN]$ from 0.7 to 3.8 M and monitored by ^1H NMR spectroscopy (see Experimental Section). At each CD_3CN concentration, the reactions are first-order in [Zr], as monitored by the disappearance of the starting material or the appearance of product, $Cp_2Zr\{N{=}C(CH_3)(CD_3)\}(CD_3CN)^+$ (**8**-d_6) or $Cp'_2Zr\{N{=}C(CH_3)(CD_3)\}(CD_3CN)^+$ (**11**-d_6). Representative kinetic plots obtained by monitoring the disappearance of the Zr–CH_3 signals of **10**-d_6 are shown in Figure 1, and pseudo-first-order rate constants k_{obs} are listed in Table II. Several control experiments were performed to verify that the THF released by the in situ preparation of **10**-d_6 does not affect the rate of the subsequent CD_3CN insertion. The k_{obs} values determined for the reaction in the presence of added excess THF (3 equiv, entry 6, Table II) and in the absence of THF (entry

(27) (a) Green, J. C.; Green, M. L.; Prout, C. K. *J. Chem. Soc., Chem. Commun.* **1972**, 421. (b) Peterson, J. L.; Lichtenberger, D. L.; Fenske, R. F.; Dahl, L. F. *J. Am. Chem. Soc.* **1975**, *97*, 6433. (c) Lauher, J. W.; Hoffman, R. *J. Am. Chem. Soc.* **1976**, *98*, 1729.

(28) The ^1H NMR spectrum of THF in CD_2Cl_2 containing CD_3CN varies slightly with temperature and $[CD_3CN]$. At −40 °C, changing $[CD_3CN]$ from 0.8 to 3.8 M shifts THF resonances from δ 3.66 and 1.80 to δ 3.64 and 1.78.

Table I. NMR Data[a,b]

compd [solvent, ^{1}H field]	^{1}H NMR chem shift	^{1}H NMR assignt	^{13}C NMR[c] chem shift	^{13}C NMR[c] assignt
$CP_2Zr(\eta^2\text{-}CH_2Ph)(CH_3CN)^+$ (1) [CD_2Cl_2, 200 MHz; ^{13}C in CD_3CN]	7.27 (m, 3 H)	*m,p*-C_6H_5	133.6 (d, 158)	*o* or *m* C_6H_5
	6.75 (m, 2 H)	*o*-C_6H_5	130.6 (d, 158)	*o* or *m* C_6H_5
	5.97 (s, 10 H)	C_5H_5	129.3 (d, 155)	*p* C_6H_5
	2.80 (s, 2 H)	CH_2Ph	126.0 (s)	ipso C_6H_5
	1.52 (s, 3 H)	NCCH_3	110.6 (d, 175)	C_5H_5
			44.1 (t, 145)	CH_2Ph
$Cp_2Zr(CH_2Ph)(THF)^+$ (2)[d] [THF-d_8, 200 MHz]	7.55 (m, 1 H)	Zr–CH_2*Ph*, *p*		
	7.4–6.85 (m, 20 H)	Zr–CH_2*Ph* and B*Ph*$_4^-$		
	6.31 (s, 10 H)	C_5H_5		
	2.66 (s, 2 H)	Zr—CH_2		
$Cp_2Zr\{N{=}C(Me)Ph\}(CH_3CN)^+$ (3) [CD_3CN, 360 MHz]	7.7–6.7 (m, 25 H)	*Ph* and B*Ph*$_4^-$	176.2	=*C*(Me)Ph
	6.30 (s, 10 H)	C_5H_5	137.8	ipso C_6H_5
	2.37 (s, 3 H)	=C(CH_3)Ph	131.9	*p* C_6H_5
	1.95 (s, 3 H)	CH_3CN liberated	129.6	*o* or *m* C_6H_5
			128.1	*o* or *m* C_6H_5
			111.8	C_5H_5
			26.5	CH_3
$Cp_2Zr\{N{=}C(Me)Ph\}(THF)^+$ (4) [CD_2Cl_2, 200 MHz]	7.6–6.7 (m, 25 H)	*Ph* and B*Ph*$_4^-$		
	6.22 (s, 10 H)	C_5H_5		
	3.68 (m, 4 H)	THF		
	2.39 (s, 3 H)	=C(CH_3)		
	1.82 (m, 4 H)	THF		
$Cp'_2Zr\{N{=}C(Me)Ph\}(CH_3CN)^+$ (5) [CD_3CN, 200 MHz]	7.65 (m, 2 H)	*o*-C_6H_5	175.9	=*C*(Me)(Ph)
	7.48 (m, 3 H)	*m,p*-C_6H_5	137.9	ipso C_6H_5
	6.17 (t, *J* = 2.6, 4 H)	C_5H_4	132.1	*p* C_6H_5
	6.08 (t, *J* = 2.6, 4 H)	C_5H_4	129.7	*m* or *p* C_6H_5
	2.41 (s, 3 H)	=C(CH_3)	128.1	*m* or *p* C_6H_5
	2.03 (s, 6 H)	$C_5H_4CH_3$	127.5	(CH)$_4$*C*Me
	1.95 (s, 3 H)	liberated CH_3CN	113.2	(*C*H)$_4$CMe
			109.6	(*C*H)$_4$CMe
			26.6	=C(CH_3)(Ph)
			15.0	$C_5H_4CH_3$
$Cp_2Zr(CH_3)(CH_3CN)^+$ [CD_2Cl_2, 200 MHz]	6.39 (s, 10 H)	C_5H_5		
	0.68 (s, 3 H)	ZrCH_3		
$Cp_2Zr(CH_3)(CD_3CN)_2^+$ (7) [CD_2Cl_2 + 2.9 M CD_3CN, 30 °C]	6.01 (s, 10 H)	C_5H_5		
	0.11 (s, 3 H)	ZrCH_3		
$Cp_2Zr(N{=}CMe_2)(CH_3CN)^+$ (8) [THF-d_8, 360 MHz]	6.20 (s, 10 H)	C_5H_5	180.9[e]	=*C*Me$_2$
	1.91 (br s, 9 H)	liberated CH_3CN + N=C(CH_3)$_2$	112.0	C_5H_5
			29.0	=C(CH_3)$_2$
			1.0	CH_3CN
$Cp_2Zr(N{=}CMe_2)(CH_3CN)^+$ (8) [CD_2Cl_2, 360 MHz]	6.12 (s, 10 H)	C_5H_5		
	1.91 (br s, 6 H)	=C(CH_3)$_2$		
	1.61 (br s, 3 H)	NCCH_3		
$Cp'_2Zr(CH_3)(THF)^+$ (9) [CD_2Cl_2, 360 MHz; ^{13}C in THF-d_8]	6.20 (m, 2 H)	C_5H_4	130.2	(CH)$_4$CMe
	6.12 (m, 2 H)	C_5H_4	116.7	(*C*H)$_4$CMe
	6.11 (m, 2 H)	C_5H_4	114.0	(*C*H)$_4$CMe
	6.07 (m, 2 H)	C_5H_4	68.2	THF
	3.49 (m, 4 H)	THF	44.5	ZrCH_3
	2.13 (s, 6 H)	$C_5H_4CH_3$	26.3	THF
	1.80 (m, 4 H)	THF	14.8	$C_5H_4CH_3$
	0.65 (s, 3 H)	ZrCH_3		
$Cp'_2Zr(CH_3)(NCCH_3)^+$ [CD_2Cl_2, 360 MHz, 30 °C]	6.19 (m, 4 H)	C_5H_4Me		
	6.15 (m, 4 H)	C_5H_4Me		
	2.19 (s, 6 H)	$C_5H_4CH_3$		
	1.38 (br s, 3 H)	NCCH_3		
	0.59 (s, 3 H)	ZrCH_3		
$Cp'_2Zr(CH_3)(NCCD_3)_2^+$ (10) [CD_3CN, 300 MHz]	5.91 (m, 4 H)	C_5H_4Me		
	5.82 (m, 4 H)	C_5H_4Me		
	2.11 (s, 6 H)	$C_5H_4CH_3$		
	0.01 (s, 3 H)	ZrCH_3		
$Cp'_2Zr(CH_3)(NCCD_3)_2^+$ (10) [CD_2Cl_2 + 3.4 M CD_3CN, 30 °C]	5.83 (m, 4 H)	C_5H_4Me		
	5.77 (m, 4 H)	C_5H_4Me		
	2.10 (s, 6 H)	$C_5H_4CH_3$		
	0.05 (s, 3 H)	ZrCH_3		

Table I (Continued)

compd [solvent, ^{1}H field]	^{1}H NMR chem shift	^{1}H NMR assign	^{13}C NMR[c] chem shift	^{13}C NMR[c] assign
$Cp_2'Zr(N{=}CMe_2)(CH_3CN)^+$ (11) [CD_2Cl_2, 360 MHz]	6.03 (m, 2 H)	C_5H_4Me	179.7	$=C(CH_3)_2$
	5.93 (m, 4 H)	C_5H_4Me	134.7	$NCCH_3$
	5.87 (m, 2 H)	C_5H_4Me	126.7	$(CH)_4CMe$
	2.06 (s, 6 H)	$C_5H_4CH_3$	112.8	$(CH)_4CMe$
	1.97 (s, 3 H)	$=C(CH_3)$	110.4	$(CH)_4CMe$
	1.92 (s, 3 H)	$=C(CH_3)$	108.4	$(CH)_4CMe$
	1.64 (s, 3 H)	$NCCH_3$	108.3	$(CH)_4CMe$
			30.2	$=C(CH_3)$
			28.1	$=C(CH_3)$
			15.2	$(CH)_4CCH_3$
			2.3	$NCCH_3$

[a] All spectra contain references for BPh_4^-.[3d] [b] Spectra taken at 23 °C unless indicated; chemical shifts in ppm and J values in Hz. [c] Multiplicity, J_{CH} from gated decoupled spectra. [d] The poor solubility of **2** in THF and its instability in CD_2Cl_2 prevent the recording of a ^{13}C NMR spectrum. [e] Nitrile carbon was not observed.

Table II. k_{obs} for Reaction of 7-d_6 and 10-d_6 with CD_3CN at 30.2 ± 0.4 °C

entry no.	compd[a]	[CD_3CN], M	k_{obs}, 10^5 s^{-1} [b]
1	10-d_6	0.75	9.25
2	10-d_6	0.83	8.65
3[c]	10-d_6	0.94	9.56
4	10-d_6	1.63	7.87
5	10-d_6	1.72	8.20
6[d]	10-d_6	1.75	8.52
7[e]	10-d_6	1.78	8.00
8	10-d_6	1.78	8.20
9	10-d_6	2.66	7.55
10	10-d_6	3.58	6.80
11	10-d_6	3.78	6.78
12[c]	10-d_6	3.87	6.75
13[f]	10-d_6	19.1	4.99
14[f]	10-d_6	19.1	5.07
15[c]	7-d_6	0.73	3.16
16	7-d_6	0.81	2.95
17	7-d_6	0.92	3.05
18	7-d_6	1.40	2.96
19	7-d_6	2.06	2.71
20[c]	7-d_6	2.89	2.78
21	7-d_6	3.28	2.83
22[f]	7-d_6	19.1	2.13

[a] Initial [Zr] = 0.03–0.08 M. [b] All data contain 10% error. [c] In the presence of the soluble salt [^{n}Bu$_4$N][BPh_4]. [d] A 3-equiv excess of THF was added. [e] **10** was used as starting material; no THF is present. [f] In neat CD_3CN.

7, see Experimental Section for sample preparation) are identical within experimental error with that determined in the presence of 1 equiv of THF (entry 8).

The data in Table II show that increasing [CD_3CN] from 0.7 to 3.8 M results in a small decrease in k_{obs} (10% for 7-d_6 and 27% for **10**-d_6). At similar [CD_3CN], the reaction of **10**-d_6 is ca. 3 times faster than that of 7-d_6. Plots of $1/k_{obs}$ vs [CD_3CN] are linear for both 7-d_6 and **10**-d_6 (Figure 2).

Irreversibility of CD_3CN Insertion. Several observations establish that the CD_3CN insertions are irreversible. Careful inspection of the NMR spectra at the end of the reaction of 7-d_6 or **10**-d_6 with CD_3CN in CD_2Cl_2 reveals that no free CH_3CN is present. Furthermore, careful integration shows that the ratio of Cp to $N{=}C(CH_3)(CD_3)$ signal intensities is 10/3 (observed ratio 3.37 ± 0.15) for the product **8**-d_6 and that the ratio of Cp' CH_3 to $N{=}C(CH_3)(CD_3)$ signal intensities is 6/3 (observed ratio 1.95 ± 0.06) for the product **11**-d_6. As exchange of free and coordinated CH_3CN is rapid for **7**, **8**, **10**, and **11**, and as exchange of the inequivalent $N{=}C(Me)_2$ groups is rapid in the presence of excess CH_3CN for both **8** and **11**, reversible CD_3CN insertion should produce **8**-d_9 and **11**-d_9, respectively, and free CH_3CN.

Intra- vs Intermolecular Insertion. Due to fast CH_3CN exchange of **7** and **10**, and poor mass spectral properties of cationic Cp_2Zr complexes, it was not possible to conduct isotope labeling experiments to distinguish between intramolecular and intermolecular pathways for eq 4. However, several observations suggest that these insertions are intramolecular. The 30 °C reaction of $Cp_2Zr(Ph)(THF)^+$ and $Cp'_2Zr(CH_3)(THF)^+$ (**9**) in CD_2Cl_2 containing 1.8 M CD_3CN yields only the intramolecular insertion products **3**-d_6 and **11**-d_6 by ^{1}H NMR spectroscopy. Less than 2% (NMR detection limit) of the cross products **5**-d_6 or **8**-d_6 is formed.[29] Similarly, the reaction of $Cp_2Zr(Ph)(THF)^+$ and $Cp'_2Zr(^nBu)(THF)^+$ in CD_3CN yields only **3**-d_6 and $Cp'_2Zr\{N{=}C(H)(CD_3)\}(CD_3CN)^+$.[3h] In this case, the butyl complex undergoes initial rapid ligand substitution and β-H elimination to generate the hydride $Cp'_2Zr(H)(CD_3CN)^+$.[3h,21] The absence of cross products $Cp_2Zr\{N{=}C(H)(CD_3CN)\}(CD_3CN)^+$ and **5**-d_6 is consistent with intramolecular CD_3CN insertion of $Cp'_2Zr(H)(CD_3CN)_n^+$ and $Cp_2Zr(Ph)(CD_3CN)_n^+$.[30]

Mechanism of CD_3CN Insertion of $(C_5H_4R)_2Zr(CH_3)(CH_3CN)_n^+$. The key experimental results relevant to the mechanism of eq 4 are as follows: (i) Over the range of [CD_3CN] studied, the reaction is slightly inhibited by added CD_3CN and plots of $1/k_{obs}$ vs [CD_3CN] are linear. (ii) The reactions are irreversible. (iii) The bis(acetonitrile) complexes **7** and **10** undergo rapid CH_3CN exchange (presumably dissociative), though the extent of CH_3CN dissociation is very small (estimated K_{eq} values <0.036 (5) and 0.23 (2) M, respectively). (iv) Complex **7** (and presumably **10**) exists as a mixture of two isomers that exchange rapidly under the reaction conditions, most likely via the mono(acetonitrile) complex.

The observation of minor rate inhibition by added CD_3CN, and Bochmann's finding that mono-RCN complexes $Cp_2Ti(CH_3)(RCN)^+$ undergo RCN insertion,[11] initially suggested a mechanism for eq 4 involving reactive mono(acetonitrile) adducts as shown in Scheme II. In this scheme, mono(acetonitrile-d_3) adduct C, formed by CD_3CN dissociation of bis(acetonitrile-d_3) isomers A and B, undergoes rate-limiting migratory CD_3CN insertion to yield the 3-coordinate azaalkenylidene species D, which is rap-

(29) In a much slower process (8 days), **3**-d_6 and **11**-d_6 undergo ligand redistribution to form an equilibrium mixture of **3**-d_6 (50%), **11**-d_6 (50%), **5**-d_6 (50%), and **8**-d_6 (50%). The scrambling only occurs after the complete disappearance of the starting material **9**.

(30) These "chemical labeling" experiments do not rigorously distinguish between intra- and intermolecular mechanisms because of differences in reactivity between $(C_5H_4R)_2Zr(R)(CH_3CN)_n^+$ species. For example, $Cp_2Zr(Ph)(THF)^+$ reacts rapidly in neat CD_3CN at 30 °C ($t_{1/2}$ < 1 min), while **9** reacts slowly ($t_{1/2}$ ca. 2 h). However, the reactivities of $Cp_2Zr(Ph)(CH_3CN)_n^+$ and $Cp'_2Zr(H)(CH_3CN)_n^+$ are probably similar.

idly trapped (negligible k_{-3}) by a second CD_3CN. However, as discussed below, this scheme is inconsistent with observations iii and iv.

The rate law for Scheme II under preequilibrium conditions is given by eqs 6–9:

$$\text{rate} = \frac{K_{eq}k_3}{K_{eq} + [CD_3CN]}[Zr] = k_{obs}[Zr] \quad (6)$$

where

$$[Zr] = [A] + [B] + [C] \quad (7)$$

$$K_{eq} = \frac{K_1K_2}{K_1 + K_2} = \frac{[C][CD_3CN]}{[A] + [B]} \quad (8)$$

$$\frac{1}{k_{obs}} = \frac{1}{K_{eq}k_3}[CD_3CN] + \frac{1}{k_3} \quad (9)$$

The preequilibrium assumption is based on the observed rapid (^1H NMR time scale) exchange between A, B, and C. The plots of $1/k_{obs}$ vs $[CD_3CN]$ allow determination of k_3, the rate constant for the insertion step, and K_{eq}, the composite CD_3CN dissociation constant.[31a] The K_{eq} values determined in this way (24 (9) M for **7** and 7.2 (4) M for **10**) are over 30 times larger than those estimated from NMR measurements as described above (<0.036 (5) M for **7** and <0.23 (2) M for **10**). For example, a value of K_{eq} = 24 M for **7** predicts a [C]/([A] + [B]) ratio of 24/1 at $[CD_3CN]$ = 1.0 M and an exchange-averaged $\delta(Zr-CH_3)$ = 0.66 ($\delta(Zr(CH_3)(CH_3CN)^+)$ = 0.68, $\delta(Zr(CH_3)(CH_3CN)_2^+)$ = 0.10). This is inconsistent with the observed $\delta(Zr-CH_3)$ = 0.13 under these conditions.[32]

Alternatively, assuming steady-state behavior for C yields a rate law (eqs 10–12) that is kinetically indistinguishable from eq 6:

$$k_{obs} = \frac{k_3\dfrac{rk_1 + k_2}{1 + r}}{k_3 + (k_{-1} + k_{-2})[CD_3CN]} \quad (10)$$

where

$$r = \frac{[A]}{[B]} \text{ (constant throughout reaction)} \quad (11)$$

$$[Zr] = [A] + [B]$$

$$\frac{1}{k_{obs}} = \frac{k_{-1} + k_{-2}}{k_3\dfrac{rk_1 + k_2}{1 + r}}[CD_3CN] + \frac{1}{\dfrac{rk_1 + k_2}{1 + r}} \quad (12)$$

In this case the intercept of the $1/k_{obs}$ vs $[CD_3CN]$ plot allows determination of $(rk_1 + k_2)/(1 + r)$, the combined rate constants for the nitrile dissociation from bis(acetonitrile-d_3) complexes A and B.[31b] The values obtained are on the order of 10^{-4} s^{-1}. These low values imply that for both **7** and **10** exchange of free (δ 1.95) and coordinated nitrile (δ <1.61, based on low-T NMR spectroscopy of **7**),[3d]

Scheme II

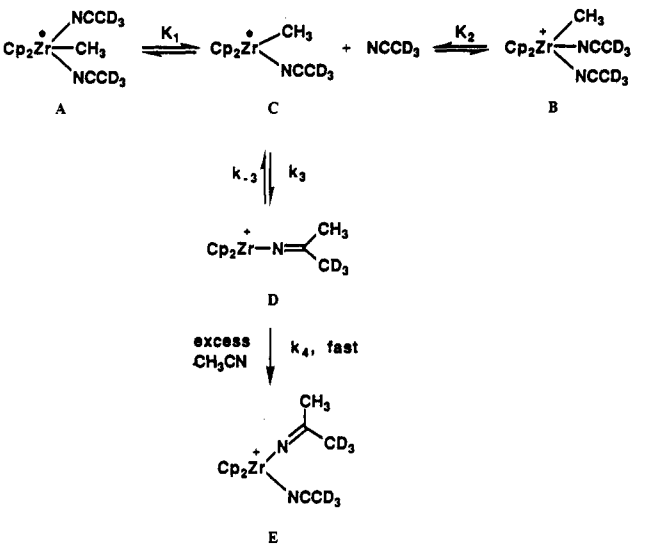

Scheme III

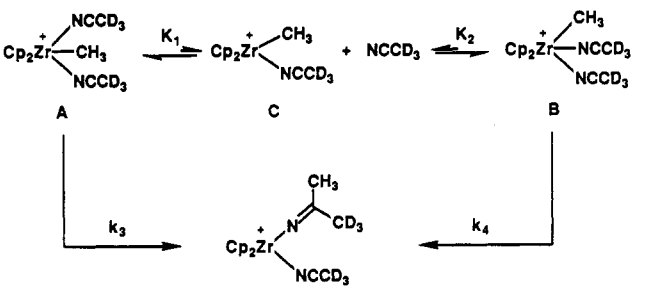

which is almost certainly dissociative, should be slow on the NMR time scale. This is inconsistent with observation iv that exchange between free and coordinated nitrile is fast on the NMR time scale for both **7** and **10**.

The observed dependence of k_{obs} on $[CD_3CN]$ is also inconsistent with mechanisms based on Scheme II and involving reversible formation of D (i.e. nonnegligible k_{-3}).[33] Furthermore, as the Zr—N=CMe_2 groups of D are likely to be equivalent ($NCMe_2$ ligand in the plane between the Cp ligands and in the central coordination site as shown) or to undergo rapid site exchange (rapid rotation about the Zr—N=CMe_2 linkage or rapid exchange of N=CMe_2 between lateral coordination sites),[34] reversible insertion

(31) (a) Assuming preequilibrium behavior for A–C, the intercept is $1/k_3$ and the slope is $1/K_{eq}k_3$ for the plot in Figure 2. The values obtained by a linear least-squares fit are k_3 = 3.13 (17) × 10^{-5} s^{-1} for **7** and 1.03 (3) × 10^{-5} s^{-1} for **10**; K_{eq} = 23.5 (88) M for **7** and 7.24 (43) M for **10**. (b) Assuming steady-state behavior for C, the intercept is $(1 + r)/(rk_1 + k_2)$ and the slope is $(k_{-1} + k_{-2})(1 + r)/[k_3(rk_1 + k_2)]$ for the plot in Figure 2. The values obtained by a linear least-squares fit are $(rk_1 + k_2)/(1 + r)$ = 3.13 (17) × 10^{-5} s^{-1} for **7** and 1.03 (3) × 10^{-5} s^{-1} for **10**; $k_3/(k_{-1} + k_{-2})$ = 23.5 (88) M for **7** and 7.24 (43) M for **10**.

(32) Moreover, on the basis of the upper limit of K_{eq} values (0.036 (5) M for **7** and 0.23 (2) M for **10**) determined by NMR measurement, one can predict a lower limit for the rate inhibition (77% for **7** and 76% for **10**) by added CD_3CN over the concentration range studied (0.7–3.8 M). This result is inconsistent with the observed small rate inhibition (10% for **7** and 27% for **10**).

(33) (a) The rate law for Scheme II, assuming steady-state behavior for D and preequilibrium behavior for A–C, is $k_{obs} = k_3k_4K_{eq}[CD_3CN]/\{(k_{-3} + k_4[CD_3CN])(K_{eq} + [CD_3CN])\}$. In this case a plot of $1/k_{obs}$ vs $[CD_3CN]$ is not linear. (b) The rate law, assuming preequilibrium behavior for A–D, is $k_{obs} = k_4K_{eq}(k_3/k_{-3})[CD_3CN]/\{K_{eq}(k_3/k_{-3} + 1) + [CD_3CN]\}$. In this case a plot of $1/k_{obs}$ vs $[CD_3CN]$ is also not linear, and k_{obs} is independent of $[CD_3CN]$ at high $[CD_3CN]$.

(34) (a) A structure with the N=CMe_2 ligand in the plane between the Cp ligands and in the central coordination site allows maximum N—Zr π bonding. Bercaw and co-workers have characterized several $Cp^*_2Sc[N=C(R)(Me)]$ complexes, which are isoelectronic with the putative species D. The observation of equivalent CMe_2 groups in the ScN=CMe_2 complex and equivalent Cp* ligands in other ScN=C(R)(Me) complexes is in accord with either a structure with the N=C(Me)(R) ligand in the plane between the Cp* ligands and in the central site or a highly fluxional structure. (b) The X ligand in d^0 Cp^*_2MX complexes lies at or close to the central coordination site (i.e. in the centroid–M–centroid plane). $Cp^*_2ScCH_3$: Thompson, M. E.; Baxter, S. M.; Bulls, A. R.; Burger, B. J.; Nolan, M. C.; Santarsiero, B. D.; Schaefer, W. P.; Bercaw, J. E. *J. Am. Chem. Soc.* **1987**, *109*, 203. $Cp^*_2YCH(SiMe_3)_2$: den Haan, K. H.; de Boer, J. L.; Teuben, J. H.; Spek, A. L.; Kojic-Prodic, B.; Hays, G. R.; Huis, R. *Organometallics* **1986**, *5*, 1726. $Me_2Si(C_5Me_4)_2NdCH(SiMe_3)_2$: Jeske, G.; Schock, L. E.; Swepston, P. N.; Schumann, H.; Marks, T. J. *J. Am. Chem. Soc.* **1985**, *107*, 8103. (c) Extended Hückel calculations predict a pyramidal structure for Cp_2TiH^+ (i.e. Ti–H ligand in a lateral site). However, this structure is only ca. 5 kcal/mol lower in energy than the triangular structure.[27c]

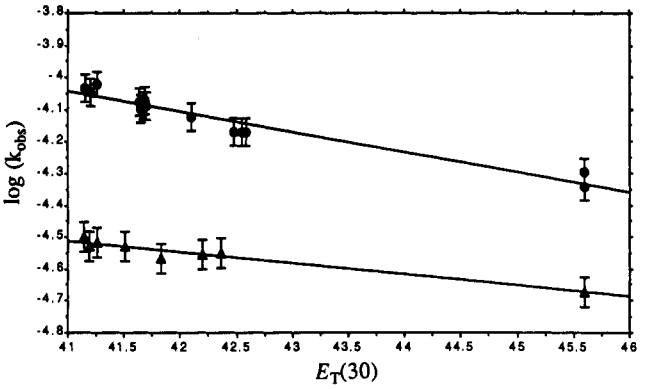

Figure 3. Plots of log k_{obs} vs $E_T(30)$: (▲) data for complex **7**-d_6; (●) data for complex **10**-d_6.

should lead to CH_3/CD_3 scrambling in reactions of **7**-d_6 or **10**-d_6 with CD_3CN. Such scrambling is not observed (observation ii).

On the basis of the above discussion we conclude that CD_3CN dissociation *is not* important for insertion of **7** or **10**. Rather, we propose that these bis(acetonitrile) complexes undergo simple migratory insertion as in Scheme III, in which one or both isomers react. The rate law for this process is given by eq 13; in the limit $(K_1 + K_2) \times [CD_3CN] \gg K_1K_2$ (which likely obtains over the entire $[CD_3CN]$ range studied due to the low K_1 and K_2 values), k_{obs} is independent of $[CD_3CN]$ (eq 14):

$$\text{rate} = \frac{(k_3K_2 + k_4K_1)[CD_3CN]}{K_1K_2 + (K_1 + K_2)[CD_3CN]}[Zr] = k_{obs}[Zr] \quad (13)$$

$$k_{obs} = \frac{k_3K_2 + k_4K_1}{K_1 + K_2} = \frac{k_3[A] + k_4[B]}{[A] + [B]} \quad (14)$$

if

$$(K_1 + K_2)[CD_3CN] \gg K_1K_2$$

The apparent minor rate inhibition by added CD_3CN is ascribed to a weak solvent effect. Acetonitrile ($\epsilon_r = 35.94$) and CD_2Cl_2 ($\epsilon_r = 8.93$) differ significantly in polarity, and the polarity of the CD_3CN/CD_2Cl_2 reaction solvent thus increases over the range of $[CD_3CN]$ studied.

One obvious way to test this proposal is to replace CD_2Cl_2 with a solvent whose polarity is similar to that of CH_3CN, so that changes in $[CH_3CN]$ would have little effect on the polarity of the mixed solvent. Unfortunately, the $(C_5H_4R)_2Zr(CH_3)(L)^+$ complexes are unstable in CH_3NO_2, alcohols, ketones, or coordinating solvents due to facile protonolysis, insertion, or ligand-exchange reactions.[35] An alternative approach is to investigate the correlation of k_{obs} with empirical solvent polarity parameters. The parameter most widely used for this purpose is the $E_T(30)$ scale of Dimroth and Reichart, which is based on the solvatochromism of a reference dye[36] and is particularly useful for characterizing the polarity of mixed solvent systems.[37] The rates of a variety of reactions correlate well with this scale. We have determined $E_T(30)$ values for the mixed solvent CH_3CN/CH_2Cl_2 over the concentration range studied as described in the Experimental Section. A linear correlation between log k_{obs} and $E_T(30)$ is observed for both **7**-d_6 and **10**-d_6 in CD_2Cl_2/CD_3CN *and* in neat CD_3CN (Figure 3). This finding is consistent with the proposal that the apparent rate inhibition by CD_3CN is due to increasing solvent polarity, although we caution against overinterpretation because of the relatively narrow range of $E_T(30)$ values.

The solvent effect may arise from several sources. One possibility is that increased solvent polarity favors the less reactive of the two bis(acetonitrile-d_3) complexes A or B and thus decreases the observed rate (eq 14). This analysis suggests that the more symmetric isomer A (with CH_3CN in the lateral sites), which should be favored at low solvent polarity, is more reactive than B. This is consistent with Erker's observation that carbonylation of Cp_2ZrMe_2 involves initial coordination of CO at a lateral site, though the transition states for these reactions may be quite different (1,3- vs 1,2-migration).[38] Unfortunately, due to rapid exchange of A and B and the similarity of their NMR spectra, it is not possible to determine the ratio [A]/[B] under the reaction conditions. An alternative possibility is that changes in solvent polarity influence ion-pairing equilibria of the ionic reactant. However, addition of $[^nBu_4N][BPh_4]$ does not strongly affect the reaction rate (entries 3, 12, 15, 20, Table II). Finally, the solvent effect may reflect differential solvation of the ground state and the rate-limiting transition state; i.e., the charge density in the transition state may be more delocalized than the ground state.[39] For comparison, a similar solvent effect was observed by Bergman, Heathcock, and co-workers for CH_3CN insertion of $(CO)_3(PPh_3)(CH_3CN)ReCH_2C(O)OEt$ in CH_3CN/benzene.[40] Interestingly, Bochmann observed that CH_3CN insertion of $Cp_2Ti(CH_3)(CH_3CN)^+$ (eq 1) in neat CH_3CN is ca. 100 times slower than expected on the basis of analogous reactions of $Cp_2Ti(CH_3)(RCN)^+$ and $(Ind)_2Ti(CH_3)(RCN)^+$ with nitriles in CD_2Cl_2.[11]

Discussion

The cationic complexes $(C_5H_4R)_2Zr(R')(CH_3CN)_n^+$ (R = H, CH_3; R' = H, CH_3, Ph), generated by oxidation of neutral $(C_5H_4R)_2Zr(R')_2$ in the presence of CH_3CN or by displacement of THF from $(C_5H_4R)_2Zr(R')(THF)^+$ complexes, react with CH_3CN via insertion to yield the azaalkenylidene complexes $(C_5H_4R)_2Zr\{N{=}C(R')(CH_3)\}(CH_3CN)^+$. Under the mild conditions studied (25–40 °C), multiple insertions, reactions involving activation of CH_3CN C–H bonds, and azaalkenylidene/CH_3CN coupling reactions are not observed. These reactions are analogous to the RCN insertions observed for the related d^0 complexes $Cp^*_2Sc(R)$, $[Cp^*_2Y(H)]_2$, and $Cp_2Ti(R)(RCN)^+$.[11-15] NMR data establish that the azaalkenylidene ligands of **3**, **4**, **8**, and **11** lie in the electronically and sterically preferred "in-plane" orientation between the two C_5H_4R ligands.

The results of kinetic studies of CD_3CN insertion of $(C_5H_4R)_2Zr(CH_3)(CD_3CN)_n^+$ complexes **7**-d_6 and **10**-d_6 and supporting solution NMR studies are best explained by the mechanism in Scheme III, in which the bis(acetonitrile) adducts are the reactive species. The slight rate inhibition

(35) The reaction of **6** in CD_3NO_2 in the presence of 4 equiv of CH_3CN is complete within 24 h and yields $Cp_2Zr(NCCH_3)(CD_2NO_2)$ (>99%) and CH_3D. ^1H NMR (CD_3NO_2): δ 6.50 (s, 10 H, C_5H_5), 2.56 (s, 3 H, coordinated CH_3CN), 2.01 (free CH_3CN), 0.16 (t, CH_3D).

(36) (a) Reichardt, C. *Angew. Chem.* **1979**, *18*, 98. (b) Reichardt, C. *Pure Appl. Chem.* **1982**, *54*, 1867 and references therein. (c) Reichardt, C. *Solvents and Solvent Effects in Organic Chemistry*; VCH: Weinheim, Germany, 1988; Chapter 7, and references therein. (d) Tang, R.; Mislow, K. *J. Am. Chem. Soc.* **1970**, *92*, 2100.

(37) (a) Langhals, H. *Angew. Chem., Int. Ed. Engl.* **1982**, *21*, 724. (b) Langhals, H. *Tetrahedron Lett.* **1986**, *27*, 339.

(38) (a) Erker, G. *Acc. Chem. Res.* **1984**, *17*, 103. (b) Tatsumi, K.; Nakamura, A.; Hofmann, P.; Stauffert, P.; Hoffmann, R. *J. Am. Chem. Soc.* **1985**, *107*, 4440.

(39) (a) Ingold, C. K. *Structure and Mechanism in Organic Chemistry*, 2nd ed.; Cornell University Press: Ithaca NY, 1969; pp 457 ff and 680 ff. (b) Hughes, E. D.; Ingold, C. K. *J. Chem. Soc.* **1935**, 244.

(40) Stack, J. G.; Doney, J. J.; Bergman, R. G.; Heathcock, C. H. *Organometallics* **1990**, *9*, 453–466.

by added CD_3CN is most likely due to the increased polarity of the solvent. This reaction mechanism differs from that for RCN insertion of $Cp_2Ti(CH_3)(RCN)^+$ complexes (eq 1), in which the mono-RCN adduct is the reactive species and formation of bis-RCN complexes does not occur. This difference is due primarily to the difference in ionic radii of Ti^{IV} and Zr^{IV} (Ti, 0.88 Å; Zr, 0.98 Å; for M^{IV} in 8-coordinate geometries).[41] For comparison, several related $Cp_2M(L)_n$ systems are known in which 18-electron complexes are favored for Zr(IV) but not for Ti(IV): e.g., $Cp_2Zr(CH_3)(PMe_3)_2^+$ vs $Cp_2Ti(CH_3)(PMe_3)^+$[3d,4a] and $Cp_2Zr(L)_3^{2+}$ vs $Cp_2Ti(L)_2^{2+}$ (L = CH_3CN, H_2O).[3e,42]

Comparison of k_{obs} values for CD_3CN insertion of 7-d_6 and 10-d_6 (Table II) indicates that the Me substituents on the Cp rings accelerate insertion by a factor of 3. As the details of the insertion step are unknown (e.g., extent of CH_3CN pivoting to a side-bonded coordination mode prior to insertion),[43] the cause of this acceleration cannot be precisely pinpointed. However, a reasonable possibility is that the developing electron deficiency at the metal center in the transition state leading from the 5-coordinate reactant to the 4-coordinate product is stabilized more by the electron-donating Cp′ ligands.[44] Steric effects arising from the Cp′ ring methyl groups should be minor for these reactions. The acceleration of CH_3CN insertion by methyl substitution of the Cp rings is consistent with Bochmann's observation that $Ind_2Ti(CH_3)(RCN)^+$ complexes insert RCN more rapidly than do $Cp_2Ti(CH_3)(RCN)^+$ complexes.[11] Recent XPS and electrochemical studies by Gassman establish that Ind is a stronger donor ligand than Cp in ruthenocene systems.[45] The influence of Cp_2M structural changes on the olefin polymerization behavior of Cp_2MX_2/aluminoxane catalyst systems, in which $Cp_2M(R)^+$ ions are believed to be active species, has been studied extensively.[7a,46] At high Al/Zr ratios, where essentially all of the Zr sites are active,[46c] polyethylene productivity is higher for the Cp'_2ZrCl_2/aluminoxane catalyst than for the Cp_2ZrCl_2/aluminoxane catalyst. This suggests that ethylene insertion (chain propagation) is faster for the Cp′ systems, consistent with our results for insertion of the model substrate CH_3CN.

While the rapid rates of the CH_3CN insertions of $(C_5H_4R)_2Zr(H)(CH_3CN)_n^+$ and $(C_5H_4R)_2Zr(Ph)(CH_3CN)_n^+$ complexes preclude the detailed kinetic studies required to assess the role of bis(acetonitrile) species, it is clear that the qualitative trend in migratory aptitude is H, Ph ≫ CH_3 ≫ η^2-CH_2Ph for these reactions. The rapid CH_3CN insertions observed for $(C_5H_4R)_2Zr(H)(CH_3CN)_n^+$ (R = H, CH_3) are consistent with the general high insertion reactivity of early-metal hydride complexes. This has been ascribed to the effective bonding of the nondirectional H 1s orbital in the bridged insertion transition state.[1d] The rapid insertions of $(C_5H_4R)_2Zr(Ph)(CH_3CN)_n^+$ species are also likely due to enhanced bonding of the Ph group in the bridged transition state due to participation of the Ph π system. NMR studies show that the Zr–Ph group in $Cp_2Zr(Ph)(THF)^+$ either is rotating rapidly or lies perpendicular to the plane between the two Cp ligands.[24] Thus, in the reactive CH_3CN complex $Cp_2Zr(Ph)(CH_3CN)_n^+$ it is likely that there is only a minimal barrier to rotation of the Ph group to an orientation in which overlap of the p orbital of the Ph ipso carbon and the LUMO of the coordinated CH_3CN is possible. In contrast, $Cp^*_2Sc(Ph)$ does not undergo facile insertion of ethylene, while the corresponding hydride and alkyl complexes do.[1d] In this case, rotation of the Ph group may be hindered by the bulky Cp* ligands. The reluctance of benzyl complex 1 to undergo insertion appears to be due to the η^2-CH_2Ph bonding mode; the Zr–Ph interaction must be disrupted to achieve a cis orientation of the migrating Zr–CH_2 bond and the coordinated CH_3CN. The observation that $(C_5H_4R)_2Zr(CH_2Ph)(THF)^+$ (R = H, CH_3) complexes catalyze ethylene polymerization suggests that cationic Zr–CH_2Ph species are not inherently unreactive in insertions and that the putative initiating $Cp_2Zr(CH_2Ph)(ethylene)^+$ species contains an η^1-CH_2Ph ligand.

Experimental Section

General Considerations. All manipulations were performed under an inert atmosphere or under vacuum with use of a Vacuum Atmospheres drybox or a high-vacuum line. Solvents were purified by initial distillation from an appropriate drying/deoxygenating agent, stored in evacuated bulbs, and vacuum-transferred to NMR tubes or reaction vessels. NMR spectra were obtained on JEOL FX-90Q, Nicolet 200, Bruker AC-300, or WM-360 instruments. IR spectra were recorded on Perkin-Elmer 238 or Matson Cygnus 25 instruments. Thermolyses were carried out with use of a VWR (Model 90T) constant-temperature bath. Elemental analyses were performed by Analytische Laboratorien or Schwarzkopf Microanalytical Laboratory, Inc. The following compounds were prepared by literature methods: $Ag[BPh_4]$,[3d] $K[CH_2Ph]$,[47] $[Cp'_2Fe][BPh_4]$,[3h] $[Cp_2Zr(CH_3)(THF)][BPh_4]$ (6),[3d] $Cp'_2Zr(CH_3)_2$,[48] Cp_2ZrPh_2,[49] and Cp'_2ZrPh_2.[50]

$Cp_2Zr(CH_2Ph)_2$. This known compound was synthesized by the following improved preparation, which utilizes $K[CH_2Ph]$ instead of $PhCH_2MgCl$.[51] A slurry of Cp_2ZrCl_2 (5.61 g, 19.6 mmol) and $K[CH_2Ph]$ (5.25 g, 40.3 mmol) in toluene (120 mL) was prepared at −78 °C. The slurry was warmed to room temperature and stirred for 75 min. The deep red slurry was filtered. The KCl precipitate was washed with 120 mL of toluene. The combined filtrate and washes were evaporated to dryness, yielding 6.92 g (89.4%) of $Cp_2Zr(CH_2Ph)_2$ as a yellow solid. This product may be further purified by recrystallization from toluene/hexane, but this was unnecessary for the synthesis of 1 and 2.

$[Cp_2Zr(\eta^2\text{-}CH_2Ph)(CH_3CN)][BPh_4]$ (1). A solution of $Cp_2Zr(CH_2Ph)_2$ (3.00 g, 7.44 mmol) in 100 mL of CH_3CN was cooled to 0 °C, and $Ag[BPh_4]$ (3.08 g, 7.22 mmol) was added via a solid addition tube over a 15-min period. The reaction mixture was stirred for 10 min at 0 °C and then warmed to 23 °C for an additional 10 min. Filtration gave a yellow/orange solution, which

(41) Shannon, R. D. *Acta Crystallogr., Sect. A* **1976**, *32*, 751.
(42) (a) Thewalt, U.; Klein, H. P. *J. Organomet. Chem.* **1980**, *194*, 297. (b) Thewalt, U.; Lasser, W. *J. Organomet. Chem.* **1984**, *276*, 341. (c) Bruce, M. R. M.; Tyler, D. R. *Organometallics* **1985**, *4*, 528.
(43) For side-on CH_3CN complexes see: (a) Wright, T. C.; Wilkinson, G.; Motevalli, M.; Hursthouse, M. B. *J. Chem. Soc., Dalton Trans.* **1986**, 2017–2019. (b) Chetcuti, P. A.; Knobler, C. B.; Hawthorne, M. F. *Organometallics* **1988**, *7*, 650–660. (c) Bullock, R. M.; Headford, C. E. L.; Hennessy, K. M.; Kegley, S. E.; Norton, J. R. *J. Am. Chem. Soc.* **1989**, *111*, 3897–3908.
(44) Gassman has quantified the electronic properties of substituted Cp ligands: (a) Gassman, P. G.; Macomber, D. W.; Hershberger, J. W. *Organometallics* **1983**, *2*, 1470. (b) Gassman, P. G.; Campbell, W. H.; Macomber, D. W. *Organometallics* **1984**, *3*, 385.
(45) Gassman, P. G.; Winter, C. H. *J. Am. Chem. Soc.* **1988**, *110*, 6130.
(46) (a) Ewen, J. A. Ligand Effects on Metallocene Catalyzed Polymerizations. In *Catalytic Polymerization of Olefins*; Keii, T. Soga, K., Eds.; Elsevier: New York, 1986. (b) Kaminsky, W.; Kulper, K.; Niedoba, S. *Makromol. Chem., Macromol. Symp.* **1986**, *3*, 377. (c) Chien, J. C. W.; Wang, B.-P. *J. Polym. Sci., Polym. Chem. Ed.* **1989**, *27*, 1539.
(47) (a) Schlosser, M. *J. Organomet. Chem.* **1967**, *8*, 9. (b) Schlosser, M.; Hartmann, J. *Angew. Chem., Int. Ed. Engl.* **1973**, *12*, 508.
(48) Couturier, S.; Tainturier, G.; Gautheron, B. *J. Organomet. Chem.* **1980**, *195*, 291.
(49) Samuel, E.; Rausch, M. D. *J. Am. Chem. Soc.* **1973**, *95*, 6263.
(50) (a) $Cp'_2Zr(Ph)_2$ was prepared by the reaction of Cp'_2ZrCl_2 with 2 equiv of PhLi at −78 °C. (b) Tainturier, G.; Fahim, M.; Trouve-Bellan, G.; Gautheron, B. *J. Organomet. Chem.* **1989**, *376*, 321. (c) Erker, G.; Czisch, P.; Benn, R.; Rufinska, A.; Mynott, R. *J. Organomet. Chem.* **1987**, *328*, 101. (d) Chen, Shoushan; Liu, Yiyin; Wang, Jitao *Sci. Sin. (Engl. Ed.)* **1982**, *25*(4), 341.
(51) (a) Fachinetti, G.; Floriani, C. *J. Chem. Soc., Chem. Commun.* **1972**, 654. (b) Fachinetti, G.; Fochi, G.; Floriani, C. *J. Chem. Soc., Dalton Trans.* **1977**, 1946. (c) Bulls, A. R.; Schaefer, W. P.; Serfas, M.; Bercaw, J. E. *Organometallics* **1987**, *6*, 1219.

was evaporated to dryness under vacuum. The resulting orange powder was recrystallized twice from warm THF (ca. 60 °C) to yield **1** as a yellow crystalline solid (1.62 g, 32.4%). IR (KBr): $\nu_{C\equiv N}$ 2300, 2268, cm^{-1}. Anal. Calcd for $C_{43}H_{40}BNZr$: C, 76.76; H, 5.99; Zr, 13.56. Found: C, 76.45; H, 6.18; Zr, 13.75.

$[Cp_2Zr(CH_2Ph)(THF)][BPh_4]$ (2). A slurry of $Cp_2Zr(CH_2Ph)_2$ (3.15 g, 7.81 mmol) and $[Cp'_2Fe][BPh_4]$ (4.17 g, 7.81 mmol) in THF (ca. 50 mL) was prepared at −78 °C and warmed to 0 °C. Within 5 min an orange solid was visible. The mixture was stirred for an additional 3.5 h at room temperature and then filtered, yielding 4.72 g (86%) of crude orange product. The solid was placed in a continuous Soxhlet-type extractor (with a small glass frit in place of a paper sample cup) and extracted with 125 mL of refluxing THF for 48 h (vacuum, pot temperature 40 °C). The resulting orange slurry was concentrated to ca. half of its original volume and filtered, yielding an orange solid. Drying overnight gave 3.40 g (62%) of **2**. Anal. Calcd for $C_{45}H_{45}BOZr$: C, 76.79; H, 6.44; Zr, 12.96. Found: C, 76.51; H, 6.35; Zr, 12.80.

$[Cp_2Zr\{N{=}C(Me)(Ph)\}(THF)][BPh_4]$ (4). Solid $Ag[BPh_4]$ (4.55 g, 10.7 mmol) was added in small portions to a slurry of Cp_2ZrPh_2 (4.00 g, 10.7 mmol) in 175 mL of CH_3CN over 2 h at 23 °C. The color of the reaction mixture gradually changed from brown to black, and a Ag mirror formed on the sides of the flask. After 4 h the mixture was filtered, yielding a pale green filtrate and a black precipitate (Ag). The precipitate was extracted with CH_3CN until the extract was colorless, and the combined filtrate/extract was evaporated to dryness under vacuum. The resulting dark green solid was extracted with Et_2O in a Soxhlet-type extractor (with a small glass frit in place of a paper sample cup) for 48 h to remove biphenyl. The remaining solid was recrystallized three times from CH_3CN and dried under vacuum, yielding beige crystalline **3** (3.35 g, 45%). IR (Nujol): $\nu_{C\equiv N}$ 2310, 2280 cm^{-1}; $\nu_{C=N}$ 1655 cm^{-1}. Complex **3** was converted to **4** by reaction with THF. A solution of **3** (0.84 g) in THF was stirred for 30 min at 23 °C. The solvent was removed under vacuum, and the resulting solid was recrystallized from THF/Et_2O to yield **4** as a white solid (0.52 g, 59% from **3**). IR (Nujol): $\nu_{C=N}$ = 1655 cm^{-1}. Anal. Calcd for $C_{46}H_{46}BNOZr$: C, 75.60; H, 6.34; N, 1.92; Zr, 12.48. Found: C, 75.32; H, 6.46; N, 1.96; Zr, 12.26.

$[Cp_2Zr(N{=}CMe_2)(NCCH_3)][BPh_4]$ (8). A solution of **6** (0.648 g, 1.04 mmol) in a mixed solvent containing 20 mL of THF and 5 mL of CH_3CN was stirred at 23 °C for 68 h and then heated to 30 °C for 28 h. The resulting bright orange solution was evaporated to dryness under vacuum, and fresh CH_3CN (ca. 10 mL) was added via vacuum transfer at −78 °C. The solution was warmed to 23 °C and evaporated to dryness under vacuum. Finally, fresh CH_3CN was added at −78 °C and the solution was warmed to room temperature and filtered. The filtrate was concentrated to ca. 2–3 mL and cooled to −78 °C, and ca. 10 mL of Et_2O was added. Warming to room temperature produced yellow solid **8**, which was collected by filtration, washed with cold Et_2O/CH_3CN, and dried under vacuum; yield 0.167 g, 25%. The low yield is due to the high solubility of **8**; in NMR tube reactions the yield is >90%. IR (KBr): $\nu_{C\equiv N}$ 2305, 2275 cm^{-1}; $\nu_{C=N}$ 1685 cm^{-1}. IR (Nujol): $\nu_{C\equiv N}$ 2300, 2270 cm^{-1}; $\nu_{C=N}$ 1680 cm^{-1}. Anal. Calcd for $C_{39}H_{39}N_2BOZr$: C, 73.56; H, 6.18; N, 4.40; Zr, 14.13. Found: C, 73.31; H, 6.11; N, 4.30; Zr, 14.05.

$[Cp'_2Zr(CH_3)(THF)][BPh_4]$ (9). A slurry of $Cp'_2Zr(Me)_2$ (6.383 g, 2.29 mmol) and $[Cp'_2Fe][BPh_4]$ (14.41 g, 2.75 mmol) in THF (200 mL) was prepared at −78 °C, warmed to 23 °C, and stirred for 3 h. The orange-brown solution was filtered and concentrated to ca. 50 mL. Addition of 150 mL of toluene at −78 °C produced a pale yellow precipitate. The mixture was warmed to 23 °C and stirred for 20 min. The volume was then reduced to ca. 160 mL and the precipitate isolated by filtration. The precipitate was washed with 10 × 10 mL of toluene, until the washings were colorless, and dried overnight under vacuum. Recrystallization from THF/hexane yielded **9** (10.2 g, 70%). Anal. Calcd for $C_{41}H_{45}BOZr$: C, 75.20; H, 6.93; Zr, 13.74. Found: C, 74.86; H, 7.04; Zr, 14.11.

$[Cp'_2Zr(CH_3)(NCCH_3)][BPh_4]$. A slurry of **9** (200 mg) in CH_3CN (5 mL) was prepared at −78 °C and was warmed to 0 °C to allow the solid to dissolve. The volatiles were removed at 0 °C. The process was repeated twice to ensure complete removal of THF. CH_2Cl_2 (5 mL) was added to the resulting solid at −78 °C via vacuum transfer, and the slurry was warmed to 0 °C for 1 min to allow the solid to dissolve. Finally, the volatiles were removed at 0 °C and the resulting light yellow foam was dried at room temperature for 30 min. The ^1H NMR spectrum of the resulting solid in CD_2Cl_2 at −80 °C showed that the solid contained 59% of the mono(acetonitrile) adduct and 41% **11**. The mono(acetonitrile) adduct decomposed at 30 °C within 12 h to a mixture of unidentified products.

$[Cp'_2Zr(CH_3)(NCCH_3)_2][BPh_4]$ (10). A 5-mm NMR tube was charged with a known quantity of **9** and evacuated on the vacuum line. CH_3CN was added at −78 °C and the solvent warmed slightly until the solid dissolved. The solvent was removed under vacuum to give a brown oil. The process was repeated to ensure a complete removal of THF. CD_2Cl_2 was added at −78 °C and the tube warmed slightly until all the solid dissolved. Volatiles were again removed under vacuum to ensure complete removal of excess CH_3CN, yielding **10** as a yellow solid. A ^1H NMR spectrum of the isolated solid at −40 °C in CD_2Cl_2 solution containing 1.8 M excess CD_3CN showed that the solid contained 2 equiv of CH_3CN.

$[Cp'_2Zr(N{=}CMe_2)(NCCH_3)][BPh_4]$ (11). A solution of **9** (1.00 g, 1.52 mmol) in a mixed solvent containing 40 mL of THF and 6 mL of CH_3CN (0.115 mol) was heated at 30 °C for 22 h. The resulting orange solution was evaporated to dryness under vacuum, and fresh CH_3CN (ca. 10 mL) was added at −78 °C via vacuum transfer. The solution was warmed to 23 °C and evaporated to dryness under vacuum. Finally, fresh CH_3CN (10 mL) was added at −78 °C and the solution was warmed to room temperature and filtered. The filtrate was concentrated to ca. 2–3 mL and cooled to −78 °C, and ca. 10 mL of Et_2O was added. Warming to room temperature produced an off-white crystalline solid, which was collected by filtration, washed with cold Et_2O/CH_3CN, and dried under vacuum, yielding 0.44 g of **11**. The filtrate was recovered and evaporated to dryness under vacuum. The residue was recrystallized from CH_2Cl_2–hexane, yielding an additional 0.22 g of **11** (total yield 71%). IR (KBr): $\nu_{C\equiv N}$ 2305, 2275 cm^{-1}; $\nu_{C=N}$ 1694 cm^{-1}. Anal. Calcd for $C_{41}H_{43}N_2BOZr$: C, 74.07; H, 6.52; N, 4.22; Zr, 13.53. Found: C, 73.70; H, 6.54; N, 3.99; Zr, 14.00.

Kinetics Measurements. Samples of **6**, **9**, or **10** were loaded into 5-mm NMR tubes equipped with valved adapters. The tubes were attached to a high-vacuum line and evacuated. A calibrated gas bulb was charged with CD_3CN at a known P (in the range 60–75 mmHg, measured by Hg manometer). The CD_3CN was transferred to the NMR tube under vacuum at −196 °C. Then the solvent CD_2Cl_2 (ca. 0.5 mL) was added via vacuum transfer at −196 °C. The tube was flame-sealed and the sample kept at −78 °C until thermolysis. Thermolyses were carried out at 30.2 ● 0.4 °C in an ethylene glycol–water (50:50) constant-temperature bath. For each measurement, the sample was removed from the bath and the reaction quenched by inserting the tube rapidly into a −78 °C bath. A ^1H NMR spectrum was recorded at −40 °C. Control experiments established that no reaction occurs at this temperature. After the spectrum was recorded, the sample was removed rapidly from the probe and inserted into the −78 °C bath and then into the constant-temperature bath at 30 °C, where the thermolysis was resumed. In this manner, the thermolyses were followed for 3–5 half-lives of each reaction. The resulting NMR spectra were plotted with use of PCNMR, which provided integration values with good reproducibility. In each case, the plot of ln ([reactant]/[reactant]$_0$) vs time or ln ([reactant]$_0$ − [product]) was linear with slope $-k_{obs}$. After each reaction, the tube was opened and the solution volume measured by syringe. The concentration of CD_3CN was calculated by assuming ideal gas behavior of CD_3CN. Results are summarized in Table II, and data analysis is described in the text.

In a control experiment, the effect of excess THF on the rate of the thermolysis was tested. A 5-mm NMR tube charged with a known quantity of **9** was evacuated on the line. CD_3CN was added via gas bulb as described above. Excess THF (3 equiv) followed by CD_2Cl_2 was added in the same manner. The reaction was monitored by ^1H NMR spectroscopy as described above. The k_{obs} value was determined as described above and was the same as that determined in the presence of 1 equiv of THF within experimental error. In a separate control experiment, **10** was generated in the absence of THF as described above, and its thermolysis in CD_2Cl_2 in the presence of CD_3CN was monitored as described above. The k_{obs} value was the same as that deter-

mined in the presence of 1 equiv of THF within experimental error.

Thermolyses in the presence of $[^nBu_4N][BPh_4]$ (0.07–0.16 M) were carried out at 30.5 ± 0.5 °C in the NMR probe, due to the poor solubility of $[^nBu_4N][BPh_4]$ at low temperature.

Calibration of Gas Bulb. To check the accuracy of the $[CD_3CN]$ measurement described above, solutions of CH_3CN in CD_2Cl_2 were prepared by gas bulb measurements and $[CH_3CN]$ was determined by the ideal gas law and by ^1H NMR integration relative to an internal standard. Bibenzyl and ferrocene were used as the standard in separate experiments. For each of three gas bulbs used in this work (volume 489.4, 214.4, 109.9 mL; pressure 60–70 mmHg), five independently prepared samples showed $[CH_3CN]_{calc}/[CH_3CN]_{obs} = 1.00 \pm 0.10$. In addition, the amount of CH_3CN added was calculated by the van der Waals equation $(P + n^2a/V^2)(V - nb) = nRT$ (where $a = 17.58$ L^2·atm·mol^{-2} and $b = 0.1168$ L·mol).[52] The calculated n from this equation showed ≤0.5% deviation from that of the ideal gas law. Thus, deviation from ideal gas behavior is negligible under these conditions.

Determination of K_{eq} by NMR Spectroscopy. The K_{eq} value for eq 5 at 30 °C for **7** and **10** was determined from the variation of $\delta(Zr-CH_3)$ (^1H NMR) vs $[CD_3CN]$ by assuming that the solvent effect on the chemical shift is minimal and δ_{mono} = 0.68 for **6** and 0.59 for **9**. Solutions of **6** or **9** in CD_2Cl_2 containing CD_3CN were prepared as described above. The ^1H NMR spectrum at 30 °C was recorded for each sample: $\delta(Zr-CH_3)_{obs}$ ($[CD_3CN]$, M) 0.14 (0.51), 0.13 (0.97), 0.12 (2.07), and 0.11 (3.07) for **6**; $\delta(Zr-CH_3)_{obs}$ ($[CH_3CN]$, M) 0.12 (0.97), 0.13 (0.99), 0.05 (3.36), and 0.05 (3.87) for **9**. For each compound a plot of $\delta(Zr-CH_3)_{obs}$ vs $(\delta_{mono} - \delta_{obs})/[CD_3CN]$ was linear. The slope of the plot equals K_{eq} (0.036 (5) M for **6** and 0.23 (2) M for **9**), and the intercept of the plot equals δ_{bis} (0.11 for **6** and 0.02 for **9**).[53]

Determination of $E_T(30)$ Values of CH_3CN/CH_2Cl_2 Mixed Solvents. The $E_T(30)$ values for CH_3CN/CH_2Cl_2 mixed solvents were determined with use of the literature procedure.[54] UV–visible spectra of Reichardt's dye in CH_2Cl_2 solutions containing 1.0, 1.5, 2.0, 2.5, 3.0, 3.5, 4.0, and 4.5 M of CH_3CN were recorded. For each solution $E_T(30)$ was determined according to the equation $E_T(30) = (28\,590$ kcal·nm$)/\lambda_{max}$. These data were fit to the equation $E_T(30) = E_D \ln([CD_3CN]/Cp^* + 1) + E_T^0(30)$, where $E_T^0(30)$ is the $E_T(30)$ value in neat CH_2Cl_2 (40.7 kcal/mol). The unknown parameters Cp^* and E_D were determined by nonlinear least-squares analysis ($Cp^* = 5.17$ (52), $E_D = 3.38$ (34)). A plot of $E_T(30)$ vs $\ln([CH_3CN]/Cp^* + 1)$ produced a straight line ($R = 0.995$), from which $E_T(30)$ values for other $[CD_3CN]$ were determined.

Acknowledgment. Early portions of this work were performed at Washington State University. We are in debt to Dr. Dennis Taylor for his generous supply of complex **6**. This work was supported by NSF Grant CHE8816445 and by DOE Grant DE-FG02-88ER13935. R.F.J. gratefully acknowledges a Sloan Foundation Research Fellowship (1989–1991) and Union Carbide Research Innovation Awards (1989, 1990).

(52) *CRC Handbook of Chemistry and Physics*, 60th ed.; CRC: Boca Raton, FL, p D-194.

(53) Drago, R. S. *Physical Methods in Chemistry*; W. B. Saunders: Philadelphia, PA, 1977; p 252.

(54) Langhals, H. *Tetrahedron Lett.* **1986**, *27*, 339.

Thermodynamic Activation Parameters in the Fluxional Behavior of $CH_2[(\eta^5\text{-}C_5H_4)M(CO)]_2(\mu\text{-}CO)$, Where M = Rh or Ir. Crystal Structure of $CH_2[(\eta^5\text{-}C_5H_4)Ir(CO)]_2(\mu\text{-}CO)$

Thomas E. Bitterwolf*

Department of Chemistry, University of Idaho, Moscow, Idaho 83843

Alessandro Gambaro and Francesca Gottardi

Department of Physical Chemistry, University of Padova, via Loredan 2, 35131 Padova, Italy

Giovanni Valle

CNR, Centro di Studio sui Biopolimeri, Department of Organic Chemistry, University of Padova, via Marzolo 3, 35131 Padova, Italy

Received November 14, 1990

The synthesis and molecular structure of $CH_2[(\eta^5\text{-}C_5H_4)Ir(CO)]_2(\mu\text{-}CO)$ is reported. ^{13}CO enrichment of the analogous rhodium complex, $CH_2[(\eta^5\text{-}C_5H_4)Rh(CO)]_2(\mu\text{-}CO)$, is also reported. Variable-temperature ^1H NMR studies of $CH_2[(\eta^5\text{-}C_5H_4)Ir(CO)]_2(\mu\text{-}CO)$ and corresponding ^1H and ^{13}C NMR studies of its rhodium analogue have been carried out. The low-temperature limiting spectra of both compounds have been fully analyzed. Coalescence temperatures for each of the three pairs of exchanging protons for the Rh and Ir complexes have been recorded, and the coalescence temperatures for the carbonyls in the rhodium compound have been recorded. Calculated $\Delta G^\ddagger$ values for the rhodium complex support a mechanism in which the ring and carbonyl motions are coupled. Comparison of $\Delta G^\ddagger$ values for the rhodium and iridium complexes reveals a substantially higher barrier for the iridium compound than for the rhodium.

The fluxional motions of a large number of dinuclear cyclopentadienyl metal carbonyl compounds have been studied in which the interconversion of cis and trans rotamers has been proposed to occur through a sequence of carbonyl bridge openings and subsequent rotations.[1] Similarly, the site exchange of terminal and bridging carbonyl groups of *trans*-$Cp_2Rh_2(CO)_2L$, where L = CO or PPh_3, has been studied by variable-temperature ^{13}C NMR, and mechanisms involving two or three bridging carbonyl groups in the exchange intermediate have been proposed.[2,3]

(1) Cotton, F. A.; Wilkinson, G. *Advanced Inorganic Chemistry*, 5th ed.; J. Wiley and Sons: New York, 1988; p 1325.

(2) (a) Evans, J.; Johnson, B. F. G.; Lewis, J.; Norton, J. R. *J. Chem. Soc., Chem. Comm.* **1973**, 79. (b) Evans, J.; Johnson, B. F. G.; Lewis, J.; Matheson, T. W.; Norton, J. R. *J. Chem. Soc., Dalton Trans.* **1978**, 626.

0276-7333/91/2310-1416$02.50/0